Modeling the thermal analysis of the uncovered solar collectors using perforated absorbent plate

Wongchai Anupong[1], Mark Treve[2,*], Iskandar Muda[3,4], I.B. Sapaev[5,6], Julio Francisco Jimenez Arana[7], Raed H. C. Alfilh[8], José Ricardo Nuñez Alvarez[9] and Morteza Almassi[10,*]

[1]Department of Agricultural Economy and Development, Faculty of Agriculture, Chiang Mai University, Chiang Mai Province, Thailand; [2]Department of School of Languages and General Education, Walailak University, Nakhon Si Thammarat, Thailand; [3]Department of Doctoral Program, Faculty Economic and Business, Universitas Sumatera Utara, Medan, Indonesia, 20222; [4]Jl. Prof TM Hanafiah 12, USU Campus, Padang bulan, Medan, Indonesia; [5]Department of Physics and chemistry, Tashkent Institute of Irrigation and Agricultural Mechanization Engineers, National Research University, Tashkent, Uzbekistan.; [6]Scientific researcher, Akfa University, Tashkent, Uzbekistan; [7]Departamento Académico De Matemática Y Física–Unsch, Universidad Nacional San Cristobal De Huamanga, Huamanga–Ayacucho, Perú; [8]Refrigeration & Air-Conditioning Technical Engineering Department, College of Technical Engineering, The Islamic University, Najaf, Iraq; [9]Energy Department, Universidad de la Costa, Barranquilla, Colombia.; [10]Department of Mechanical Engineering, Novin University, Ardebil, Iran

Abstract

Uncovered solar collectors using perforated absorbent plates are a variety of reception collectors that are used for solar heating of air for consumption in air conditioning systems and dryers. The thermal performance of these collectors is subject to various factors including diameter and step holes, air suction velocity and solar radiation. Using modeling, a proper evaluation of the effect of each of these parameters on the thermal performance of the collector can be obtained. In this paper, by using heat transfer and energy balance modeling in different components of the sample collector, the effect of each of these parameters is estimated by using the preheatment of building air, thermal efficiency and output temperature of the collector according to the parameters of solar radiation, air suction velocity, diameter and step of the holes of the absorbent plate. Also, the efficiency of heat exchange of perforated plates is estimated for air suction velocity, diameter and step of holes. The results show that increasing the suction rate of air and solar radiation increases the thermal efficiency of the collector. Also, efficiency of the heat exchange (ε_{HX}), which decreases with increasing suction speed, is due to the decrease in the output temperature of the collector because of the increase in the amount of inlet air to it, increasing the suction rate from 60 m/h to 160 m/h reduces the efficiency of the heat exchange by 30%.

Keywords: output temperature; thermal efficiency; thermal performance; modeling; perforated absorbent plate; solar collector

*Corresponding authors:
trevemark@yahoo.com;
m.almassi36@yahoo.com

Received 25 August 2022; revised 9 October 2022; accepted 31 October 2022

International Journal of Low-Carbon Technologies 2022, 17, 1435–1442

https://doi.org/10.1093/ijlct/ctac119 Advance Access publication 31 December 2022

1 INTRODUCTION

Solar thermal energy as an endless and clean source has been considered for many years for various applications. Solar collectors are heat exchangers that convert the solar radiant energy into thermal energy for various uses including hot water supply [1–3] or air heating. Unglazed transpired collectors (UTC hole) solar collectors are a justifiable technology for using solar thermal energy for commercial and household applications. Using these collectors can preheat the air and reduce the heating load of the building [4–6]. Also, this type of collector is used in the drying processes of crops [7], absorbent cooling [8], preheating the inlet air of the Boiler [9] and photovoltaic-thermal system [10].

Currently, uncovered solar collectors with the perforated absorbent plate are commercially marketed [11–13]. Uncovered solar collectors using perforated absorbent plates have a very simple system. The air passes through the holes created on an absorbent plane exposed to the sun's radiation and heats up. The suction of the air through these holes was done by a sucker fan. So far, a majority of studies have been conducted on UTC systems on commercial and laboratory scales. Studies on heat transfer drops were conducted by Ekoja *et al*. [14]. They considered the drops in heat transfer in their model. They also showed that uniform air suction fixed the thickness of the hydrodynamic boundary layer and thermal boundary layer during the collector.

Researchers [15, 16] obtained relationships related to the efficiency of heat exchange and pressure drop using the results of several experiments. Using 2D computational fluid dynamics, Ganwick *et al*. obtained the efficiency of heat exchange for UTC, which Van Decker *et al*. [17] extended to the experimental study presents an improved thermal analysis performance for the conventional unglazed transpired collector (UTC). Decreasing radiation and convection heat transfer loss to the environment and increasing heat transfer coefficient of the passing air with, first: Adding fifteen-wire mesh layers as an alternative of the perforated absorbing plate. Bokor et al. [18] presented a nocturnal passive cooling by transpired solar collectors. Alayi et al. [19] presented thermal and environmental analysis solar water heater system for residential buildings. Gao et al [20] conducted an energy and exergy analysis of a glazed solar preheating collector wall with non-uniform perforated corrugated plate.

Liu et al [21] presented an operating performance of a solar/air-dual source heat pump system under various refrigerant flow rates and distributions. Motahar [22] presented that a thermal performance of UTCs is a function of various parameters including incident solar radiation, air approach velocity, diameter and pitch of perforations. Modeling predicts the thermal performance of UTCs over a wide range of design and operating conditions. Saini et al. [23] used the techno-economic analysis of an exhaust air heat pump system assisted by unglazed transpired solar collectors in a Swedish residential cluster.

Although the use of laboratory methods or computational fluid dynamics to understand how heat transfer in unmasked solar collectors has led to the development of multiple heat transfer relationships for these systems, these methods are very costly and are not suitable for quick design or initial estimates. An inexpensive and reliable model that has been verified using laboratory results and can express practical results for the design of this system has so far been of little attention.

In this paper, the thermal performance of an unmasked solar collector with a perforated absorbent plate is modeled using building air preheating based on energy balance equations using MATLAB software. Such an earlier applied study has rarely been conducted. First, the proposed model is confirmed by experimental data; then thermal efficiency, output temperature and heat exchange efficiency under different conditions of collector design and function are to be investigated.

2 MATERIALS AND METHODS

2.1 Problems and assumptions

In this paper, a solar collector without perforated covering, which includes a sun absorbent perforated plate, is installed on a southern wall to preheat the inlet air of the building. The air is suctioned from the holes into the collector's chamber (Plenum) and eventually enters the heating system of the building. In the modeling of this UTC, the following assumptions are applied:

1. The air inside the chamber only moves vertically and the collector is assumed to be two-dimensional.
2. The absorbent plate has holes with a triangular arrangement. (Figure 1b).
3. The air temperature inside the chamber and the temperature of the absorbent plate are uniform.
4. Thermophysical properties of air follow the equation $AT^4 + BT^3 + CT^2 + DT + E$, where temperature T is obtained from Table 1 in terms of Kelvin and constants A, B, C, D and F. Also, the air density (ρ) is obtained from the relationship $\rho = 360.7782\ T^{-1.00336}$ (kg/m^3), where T is the temperature in Kelvin [20]. Using energy equations and heat transfer on the collector and wall, the thermal efficiency and output temperature of the collector are modeled based on modifiable parameters.

2.2 Energy equations

Different mechanisms of heat transfer on the solar collector, which are effective in modeling its performance, are shown in Figure 1a.

Heat is transmitted outward from within the room by conductance ($q_{cond,\ w}$), part of which is exchanged through radiation ($q_{rad,\ w\text{-}c}$) with the absorbent plate, and the other part is given to the chamber air through displacement ($q_{conv,\ w\text{-}p}$). The energy balance on the wall is derived from equation 1:

$$q_{cond,w} = q_{conv,w-p} + q_{rad,w-c}. \quad (1)$$

Table 1. *Thermo-physical properties of air [20, 24, 25].*

	A	B	C	D	E
C_P (J/kg.K)	1.933×10^{-10}	-7.999×10^{-7}	1.141×10^{-3}	-4.489×10^{-1}	1.058×10^{3}
ν (m²/s)	0	-1.156×10^{-14}	9.573×10^{-11}	3.760×10^{-8}	-3.44810^{-6}
k (W/m.K)	0	1.521×10^{-11}	-4.857×10^{-8}	1.018×10^{-4}	-3.933×10^{-4}
α(m²/s)	0	0	9.102×10^{-11}	8.820×10^{-8}	-1.065×10^{-5}

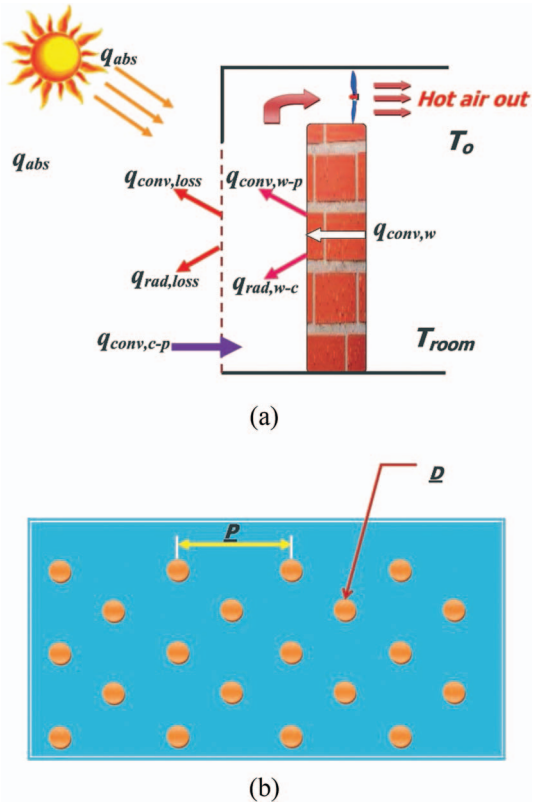

Figure 1. *(A) Heat transfer mechanisms on the UTC; (B) triangular arrangement of holes on a part of the absorbent plate.*

Also, according to Figure 1, the energy balance on the absorbent screen will be as follows:

$$q_{abs} + q_{rad,w-c} = q_{conv,c-p} + q_{conv,loss} + q_{rad,loss}. \quad (2)$$

That is, the total solar energy absorbed by the absorbent plate (q_{abs}) and the radiant heat energy received from the wall ($q_{rad,\ w\text{-}c}$) is equal to the total heat energy received by moving from the perforated plate to the chamber air ($q_{conv,c\text{-}p}$), the loss of heat energy through the displacement to the ambient air ($q_{conv,loss}$) and the loss of heat energy through radiation to the sky ($q_{rad,\ loss}$). The heat absorbed from the sun's radiation is obtained by the collector from equation 3.

$$q_{abs} = \alpha_c I_T A_s, \quad (3)$$

where α_c is the absorption coefficient of the collector's absorbent plate, I_t is the rate of solar radiation and $A_s = (-1)$ A is the area of the absorbent surface or the total area of the collector's surface (A) minus the area of the holes.

The porosity of the perforated absorbent plate (σ) is defined by equation 4 [14]:

$$\sigma = 0.907 \left(D/P\right)^2, \quad (4)$$

where P is the step and D is the diameter of the holes. The radiant energy exchanged between the wall and the collector is as follows [25]:

$$q_{rad,w-c} = \sigma_{sb} A \left(T_w^4 - T_c^4\right) / \left(1/\varepsilon_w + 1/\varepsilon_c - 1\right), \quad (5)$$

where $\sigma_{sb} = 5.67 * 10^{-8}$ (W/m². k⁴) Stephen–Boltzmann constant, T is absolute temperature and ε is the issuance coefficient.

The airflow through the collector's holes to the chamber causes the displacement heat to be transferred, which is the equation of displacement as follows:

$$q_{conv,c-p} = \dot{m} C_p \left(T_p - T_a\right) = \dot{m} C_p \varepsilon_{HX} \left(T_c - T_a\right), \quad (6)$$

where Tp is the air temperature in the enclosure, Ta is the ambient air temperature, Tc is the collector temperature and cp is the special heat of the air. Also, mc = VsA where Vs is the speed of air suction towards the collector.

In equation 6, ε_{HX} is the efficiency of heat exchange and equation 7 can be obtained as [14] follows:

$$\varepsilon_{HX} = \frac{T_p - T_a}{T_c - T_a} = 1 - \exp\left(-\frac{kNu_D\left(1-\sigma\right)}{D_\rho V_s C_p}\right), \quad (7)$$

where k is the thermal conductivity coefficient of the air. For $5\% < \sigma < \%1.0$ and $2000 < Re_D < 100$, equation 8 offers a formula for Nusselt in holes [14]:

$$Nu_D = 2.75\left[\left(\frac{P}{D}\right)^{-1.2} Re_D^{0.43} + 0.011\sigma Re_D\left(\frac{U_\infty}{V_s}\right)^{0.48}\right], \quad (8)$$

where U_∞ and V_s are wind speed and air suction speed, respectively, toward collector and Re D Reynolds number is based on the air speed in the hole, which is defined by the equation $Re_D = V_h D/v$ (.) $V_h = V_s/\sigma$ and the rate of drop caused by the transfer heat

from a collector with a wavy plate is obtained from the following equations [14]:

$$\begin{matrix} q_{conv,loss} = \frac{Nu_{loss}k}{H}A_s\left(T_c - T_a\right) \\ Nu_{loss} = 0.82\frac{\rho C_p U_\infty \nu}{kV_s}C_f \end{matrix}, \quad (9)$$

where in the air kinematic vlescetic and C_f wave coefficient is the shape of the plate, which is considered equal to one for flat plates. The collector's radiant drops to the environment can be obtained from equation 10 [25, 26]:

$$\begin{matrix} q_{red,loss} = \varepsilon_c\sigma_{sb}A\left(T_c^4 - T_{sur}^4\right) \\ T_{sur}^4 = 0.5\left(T_{sky}^4 + T_{gr}^4\right) \\ T_{sky} = 0.0552T_a^{1.5}, T_{gr} \cong T_a \end{matrix}. \quad (10)$$

The exterior surface of the wall receives heat from the inside of the room through conduction, and the conductive heat transfer through the wall is derived from equation 11 [26]:

$$q_{cond,w} = U_{cond.w}A\left(T_{room} - T_w\right). \quad (11)$$

Also, the heat transmitted from the wall is obtained by displacement from equation 12 [25]:

$$Nu_H = \begin{cases} q_{conv,w-p} = \frac{kNu_H}{H}A(T_w - T_p) \\ 0.664\,\mathrm{Re}_H^{0.5}\mathrm{Pr}^{0.333}\;\mathrm{Re}_H < 5\times10^5 \\ \left(0.037\mathrm{Re}_H^{0.8} - 871\right)\mathrm{Pr}^{0.333}\;\mathrm{Re}_H > 5\times10^5 \end{cases}. \quad (12)$$

To obtain the temperature of the hot air output from the solar collector (T_o), the heat transmitted by moving from wall to air of the chamber is considered as follows [26]:

$$q_{conv,w-p} = \dot{m}C_p\left(T_oT_p\right). \quad (13)$$

The collector's thermal efficiency is defined as the useful heat obtained from the collector to the incoming solar energy, which will be derived from the equation 14:

$$\eta = \frac{\dot{m}C_p\left(T_o - T_a\right)}{I_TA}. \quad (14)$$

The above energy equations are solved based on the algorithm presented in Figure 2 using MATLAB software and the collector temperature and wall are obtained.

2.3 Model verification

The experimental results of the performance of a sample perforated glass collector are presented by NSTF 1 [27] in Figure 1 increasing the air temperature ($T_p - T_a$) in terms of solar radiation for the intensity of currents 130,72 and 20 m/h.

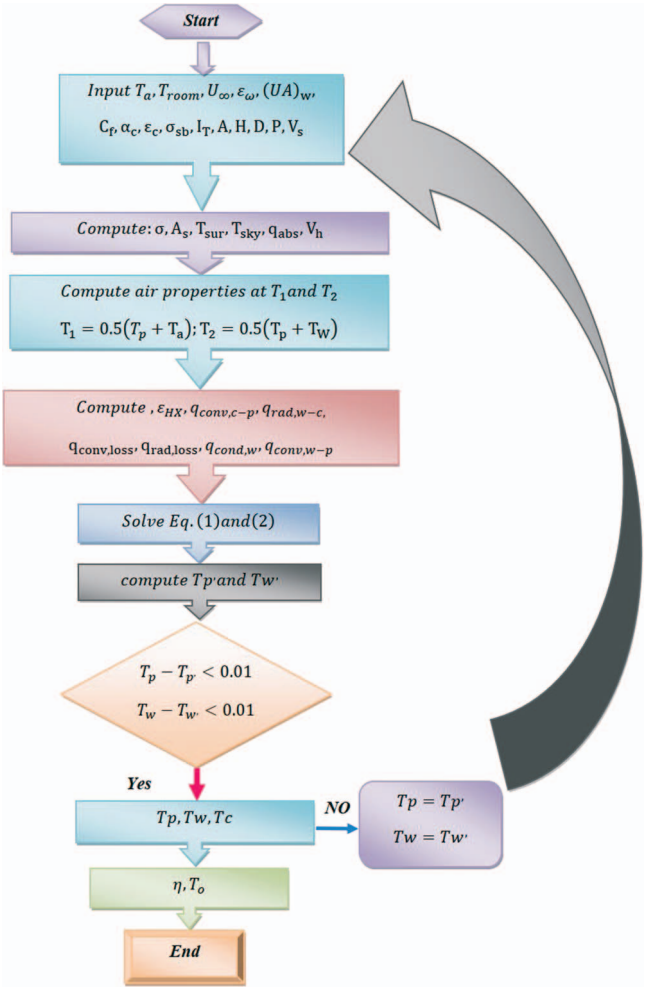

Figure 2. *Modeling algorithm.*

Room air temperature is kept constant at 22°C. NSTF tests were performed at room temperature. The results of the proposed model have been shown compared with the laboratory results in Figure 3. As can be seen from Figure 3, there is very good coordination between the test results and the present model at high suction speeds, but at low suction speeds due to the increase in the drops caused by the free-movement heat transfer, the test results show a lower temperature increase. Therefore, the present model does not provide acceptable results for suction speeds less than 72 m/h.

3 RESULTS

In this section, the results of modeling the performance of the sample solar collector are given. The following parameters and Table 2 are used in modeling:

T_{room} = 20 °C, U = 1.2 m/s, T_a = 10 °C, $(UA)_w$ = 1, C_f = 1, ε_c = 0.9.

When a parameter changes, the rest is kept steady.

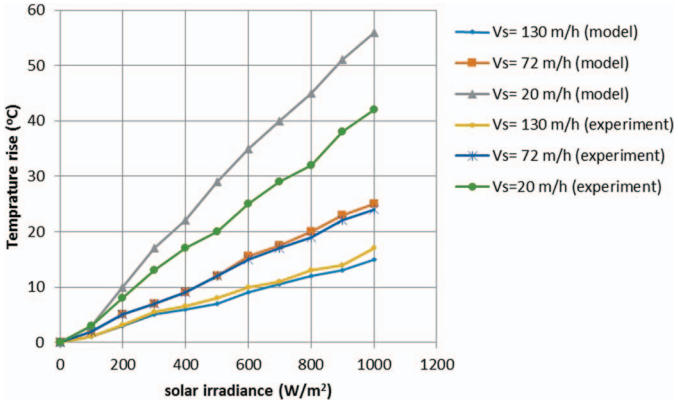

Figure 3. *Increasing the temperature in the collector in terms of solar radiation.*

Table 2. *Sample collector specifications [26].*

Parameter	Quantity
Collector height	2.44 m
Collector width	1.83 m
Chamber depth	0.0762 m
Hole diameter	0.00159 m
Step holes	0.0214 m
Porosity	0.5%

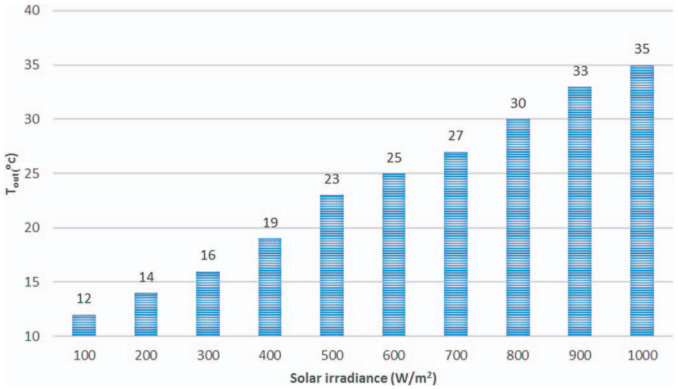

Figure 4. *Output temperature in terms of solar radiation.*

3.1 Investigating the effect of sunlight on the function of UTC

Changes in the temperature of the exhaust air from the collector (Tout) with the amount of solar radiation in Figure 4 are shown. This diagram is plotted for Vs = 72 m/h, D = 1.59 mm and P = 15.1 mm. As Figure 4 implies, increasing the amount of solar radiation means increasing the inlet heat to the collector and thus increasing its output temperature. In Figure 4, due to the ambient temperature of 10°C and the significant increase in temperature, UTC has a high potential for drying agricultural products.

The thermal efficiency of UTC is shown by the assumptions mentioned of Figure 4 in Figure 5. As can be seen from Figure 5, thermal efficiency increases with increasing rate of solar radiation,

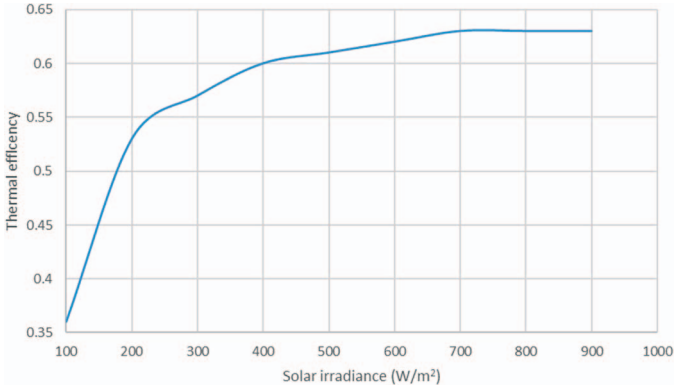

Figure 5. *Thermal efficiency in terms of solar radiation.*

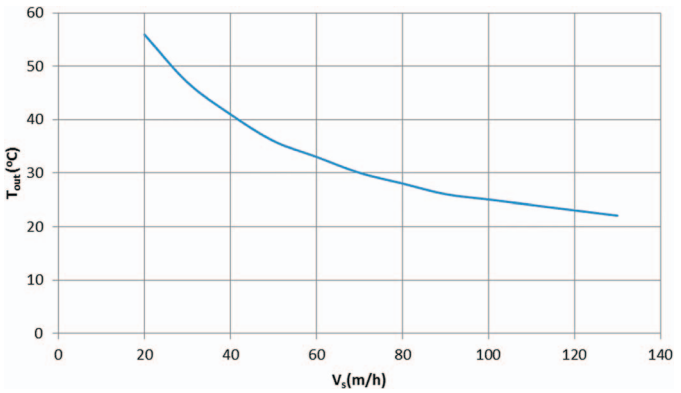

Figure 6. *The output temperature of the collector in terms of air suction speed.*

which continues first with a high slope and then with a slow slope. By increasing the amount of solar radiation entering the collector, its output temperature also increases, which is lower than the input energy. In fact, with the increase in the rate of energy input, the heat transfer drops have increased.

3.2 The effect of air suction velocity on the function of UTC

The effect of air suction velocity on the collector's performance in this section has been investigated. Figure 6 shows the temperature of the collector's outlet air in terms of the speed of the air suction towards the collector. This shape is plotted by constantly placing radiation intensity equal to I_T = 800 W/m², the ambient temperature of T_a = 10 °C and values in Table 2. By increasing the suction speed of the air towards the collector, more air passes through the holes and has less opportunity to warm up, resulting in higher suction speeds, and the temperature of the outlet air is lower than the collector. For example, by increasing the suction speed of the air to the collector from 40 to 60 m/h, the collector's output temperature drops about 10°C.

Figure 7 shows the efficiency of the heat exchange (ε_{HX}), which decreases with increasing the suction speed, which is due to the decrease in the output temperature of the collector due to the

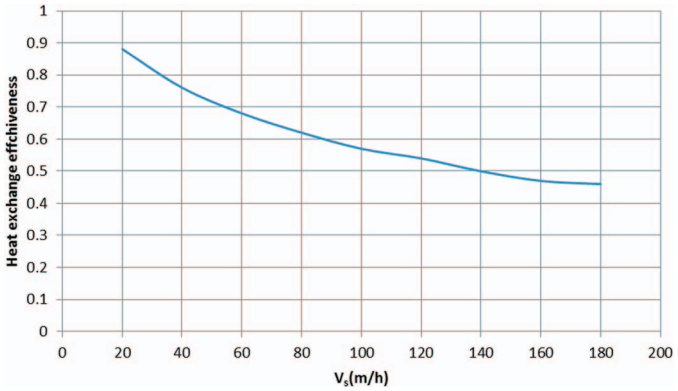

Figure 7. *Changes in the efficiency of heat exchange with air suction speed.*

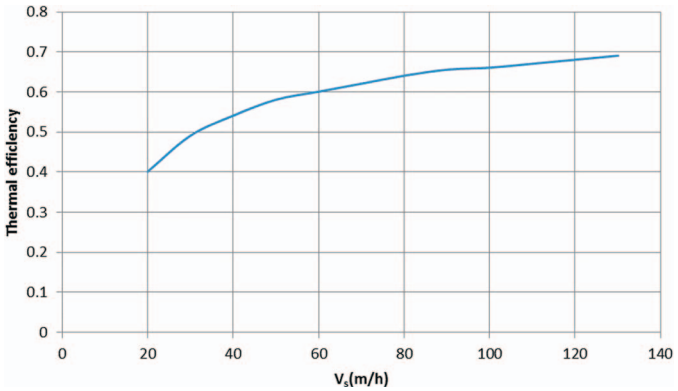

Figure 8. *Changes in thermal efficiency with air suction rate.*

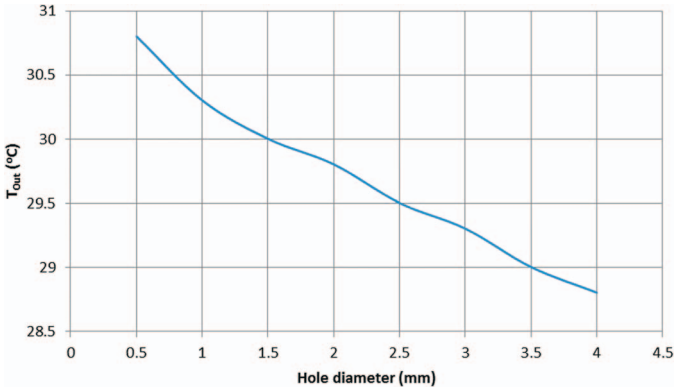

Figure 9. *Changes in the output temperature of the collector with the diameter of the holes.*

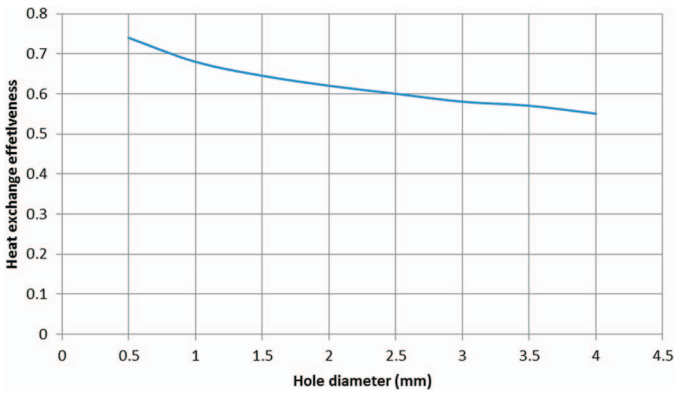

Figure 10. *Changes in the efficiency of heat exchange with the diameter of holes.*

increase in the amount of inlet air to it, increasing the suction rate from 60 to 160 m/h reduces the efficiency of the heat exchange by 30%.

In Figure 8, according to the assumptions applied to Figures 6 and 7, the thermal efficiency of the collector in terms of the speed of air suction towards the collector is shown. By increasing the suction speed, the mass discharge of the air increases and the working temperature of the collector decreases, which reduces heat transfer drops and increases the heat efficiency. Up to an approximate speed of 60 m/h, the increase in efficiency occurs fairly with a steep slope, after which the slope of the increase in returns will be softened, which is consistent with the results provided by the reference [28].

3.3 Investigation of the effect of absorbent plate holes diameter on UTC function

Figure 9 shows the effect of changing the diameter of the holes of the absorbent plate from 0.5 to 4.0 mm on the output temperature of the collector. This shape is plotted assuming that the hole step is equal to P = 21.4 mm and I_T = 800 W/m^2..

Since by increasing the diameter of the holes in the plate, the speed of the air passing through the holes decreases, the noslet number decreases, and the heat transfer to the air decreases, so the temperature of the outlet air decreases.

Figure 10 shows the efficiency of heat exchange in terms of hole diameter variations. Due to the relationship of 8 and the reduction of diameter, porosity and noslet number, the HX value decreases.

Figure 11 shows the effect of changing the diameter of the holes of the absorbent plate on the thermal efficiency. By increasing the diameter of the holes in the plate, it is generally observed to decrease in thermal efficiency. Since by increasing the diameter of the holes, the speed of the air passing through the holes decreases, the noslet number decreases and the heat transfer to the air decreases, so the heat efficiency decreases. By changing the diameter of the holes of the absorbent plate from 0.5 to 4.0 mm, the heat efficiency of UTC decreases by about 10%.

3.4 Investigation of the effect of step and porosity of adsorbent plate holes on UTC function

Figure 12 shows the temperature of the exhaust air from the collector in different steps of the holes, assuming the constant diameter of D = 1.59 mm and I_T = 800 W/m^2. By reducing the step size of the holes, the temperature of the outlet air decreases. There is no noticeable reduction in Tout between the 10 and

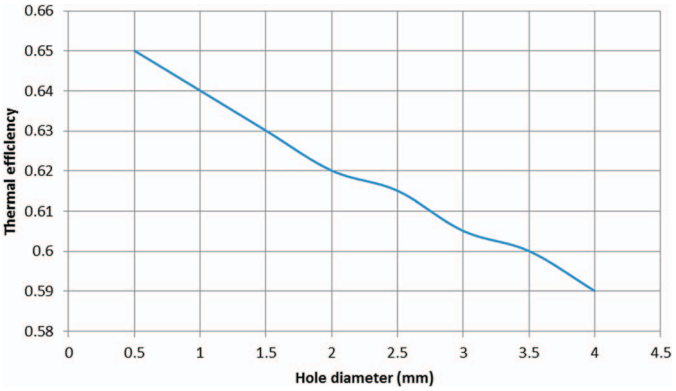

Figure 11. *Changes in heat efficiency in terms of the hole diameter.*

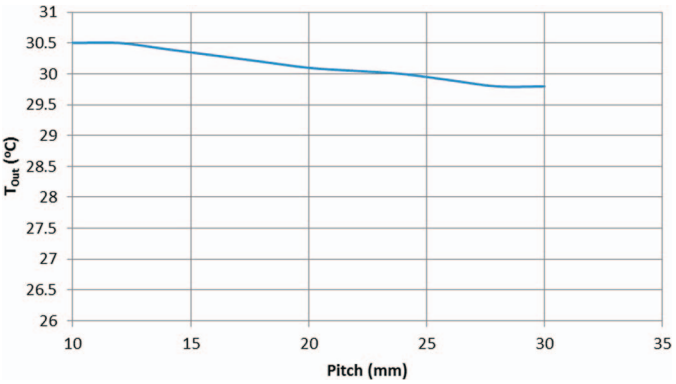

Figure 12. *Changes in the output temperature by step of holes.*

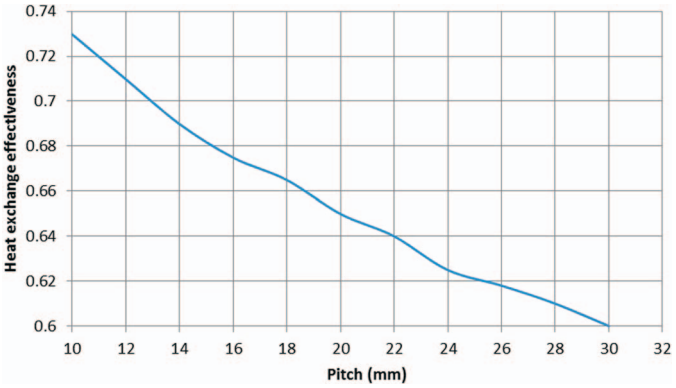

Figure 13. *Changes in the efficiency of heat exchange with the step of holes.*

12 mm steps, but then the temperature drop occurs with a greater slope. According to Figure 12, with a threefold increase in step, the output air temperature decreases by less than 3%. The efficiency of heat exchange decreases with increasing the step size of the holes as shown in Figure 13. According to this form, the step increase of holes has more effect on the HX value, so that in the given step change interval, the efficiency of heat exchange is about 18%, due to the reduction of Nusselt number.

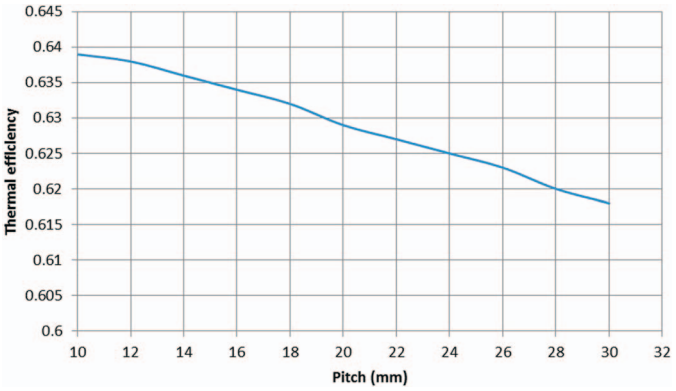

Figure 14. *Changes in UTC thermal efficiency by step of holes.*

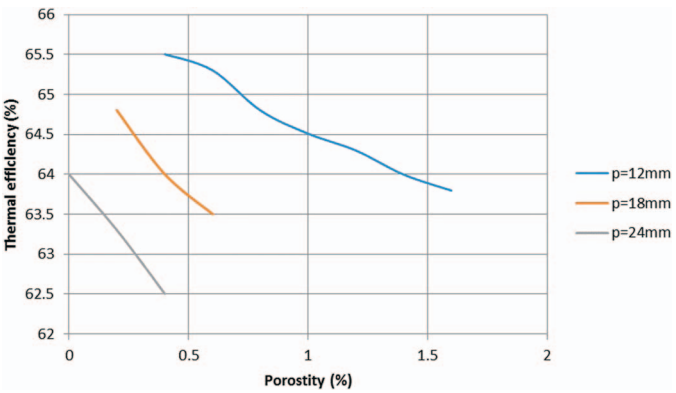

Figure 15. *Changing the heat efficiency of UTC by the porosity of the absorbent plate.*

Changes in the thermal efficiency of the collector with the step of the holes are shown in Figure 14. Although step increase has reduced thermal efficiency, its effect is very low compared to other parameters. Figure 14 shows that by increasing the step of the holes from 10 to 30 mm, the thermal efficiency decreases by less than 3%. As the holes step up, the hot spots are further away from the holes and heat loss increases due to radiation, thus reducing the efficiency of the collector's heat.

Figure 15 shows the porosity effect of the absorbent plate on the collector's thermal efficiency. According to this form, in a fixed step, the increase in porosity has little effect on reducing the efficiency, so the increase in porosity from 0.4% to 1.6% is only associated with a 2% reduction in thermal efficiency. Also, by increasing the step of the holes, the porosity of the absorbent plate has decreased but its effect on the change of efficiency is low.

4 CONCLUSIONS

In this paper, a model based on energy balance equations and heat transfer was presented to predict the thermal performance of an uncovered solar collector with a perforated absorbent plate,

with changes in the important parameters of collector design. The results of modeling showed the following:

(A) The present model provides acceptable results for suction speeds greater than 72 m/h to predict the thermal performance of the tested solar collector.

(b) The rate of solar radiation has a great effect on the performance of the collector so that by increasing the radiation, the output temperature and the efficiency of the collector increase significantly.

(C) The collector at high suction speeds (high mass flow intensity) shows better thermal efficiency, although at these speeds the efficiency of heat exchange and output temperature decreases.

(D) By increasing the diameter of the holes of the absorbent plate in a fixed step, the nolset number decreases and the efficiency of heat exchange and output temperature decreases.

(E) Increasing the step of holes for a constant diameter reduces the heat exchange coefficient and output temperature. Also, although step increase has reduced thermal efficiency, its effect is very low compared to other parameters.

(F) In a fixed step, increasing porosity has little effect on reducing efficiency. By increasing the step of the holes, the porosity of the adsorbent plate decreases, but its effect on the change of efficiency is low.

As for future works, the discussion studied in this work was on the solar section of these resources. According to these applications, the following items can be considered in future works: (1) optimization with intelligent algorithms for maximum absorption of solar heat and (2) investigation for the combined cooling, heating and power.

REFERENCES

[1] Alayi R, Sevbitov A, Assad MEH *et al.* Investigation of energy and economic parameters of photovoltaic cells in terms of different tracking technologies. *Int J Low Carbon Technol* 2022;**17**:160–8.

[2] Alayi R, Mohkam M, Monfared H *et al.* Modeling and analysis of energy/exergy for absorber pipes of linear parabolic concentrating systems. *Int J Photoenergy* 2021;**2021**7929756. https://doi.org/10.1155/2021/7929756.

[3] Alayi R, Harasii H, Pourderogar H. Modeling and optimization of photovoltaic cells with GA algorithm. *J Robotics Control* 2021;**2**:35–41.

[4] Gao M, Fan J, Furbo S, Xiang Y. Energy and exergy analysis of a glazed solar preheating collector wall with non-uniform perforated corrugated plate. *Renew Energy* 2022;**196**:1048–63.

[5] Alayi R, Jahangiri M, Najafi A. Energy analysis of vacuum tube collector system to supply the required heat gas pressure reduction station. *Int J Low Carbon Technol* 2021;**16**:1391–6.

[6] Alayi R, Kumar R, Seydnouri SR *et al.* Energy, environment and economic analyses of a parabolic trough concentrating photovoltaic/thermal system. *Int J Low Carbon Technol* 2021;**16**:570–6.

[7] Rashidi M, Arabhosseini A, Samimi-Akhijahani H *et al.* Acceleration the drying process of oleaster (*Elaeagnus angustifolia* L.) using reflectors and desiccant system in a solar drying system. *Renew Energy* 2021;**171**: 526–41.

[8] Mustafa AA, Noranai Z, Imran AA. Solar absorption cooling systems: a review. *J Therm Eng* 2021;**7**:970–81.

[9] Han Y, Sun Y, Wu J. A low-cost and efficient solar/coal hybrid power generation mode: integration of non-concentrating solar energy and air preheating process. *Energy* 2021;**235**:121367.

[10] Alayi R, Jahanbin F, Aybar HŞ *et al.* Investigation of the effect of physical factors on exergy efficiency of a photovoltaic thermal (PV/T) with air cooling. *Int J Photoenergy* 2022;**2022**9882195. https://doi.org/10.1155/2022/9882195.

[11] Abo-Elfadl S, Yousef MS, El-Dosoky MF, Hassan H. Energy, exergy, and economic analysis of tubular solar air heater with porous material: an experimental study. *Appl Therm Eng* 2021;**196**:117294.

[12] Alwan NT, Majeed MH, Khudhur IM *et al.* Assessment of the performance of solar water heater: an experimental and theoretical investigation. *Int J Low Carbon Technol* 2022;**17**:528–39.

[13] Aldawoud A, Aldawoud A, Aryanfar Y *et al.* Reducing PV soiling and condensation using hydrophobic coating with brush and controllable curtains. *Int J Low Carbon Technol* 2022;**17**:919–30.

[14] Ekoja M, Onyegegbu S, Ekechukwu OV. Theory of a glazed transpired solar collector in natural convection mode. *J Solar Energy Eng* 2022;1–23.

[15] Pop OG, Berville C. 2021. Mathematical modelling of unglazed transpired solar collectors. In *The 2021 10th International Conference on Energy and Environment (CIEM)*. IEEE. 1–5.

[16] Abed FM, Zaidan MH, Hasanuzzaman M *et al.* Modelling and experimental performance investigation of a transpired solar collector and underground heat exchanger assisted hybrid evaporative cooling system. *J Build Eng* 2021;**44**:102620.

[17] Mahmood AJ. Experimental study for improving unglazed solar system. *Cogent Eng* 2021;**8**:1961564.

[18] Bokor B, Akhan H, Eryener D *et al.* Nocturnal passive cooling by transpired solar collectors. *Appl Therm Eng* 2021;**188**:116650.

[19] Alayi R, Khalilpoor N, Heshmati S *et al.* Thermal and environmental analysis solar water heater system for residential buildings. *Int J Photoenergy* 2021;**2021**:1–9. https://doi.org/10.1155/2021/6838138.

[20] Alayi R, Kasaeian A, Atabi F. Thermal analysis of parabolic trough concentration photovoltaic/thermal system for using in buildings. *Environ Prog Sustain Energy* 2019;**38**:13220.

[21] Liu Z, Wang Q, Wu D *et al.* Operating performance of a solar/air-dual source heat pump system under various refrigerant flow rates and distributions. *Appl Therm Eng* 2020;**178**:115631.

[22] Motahar S. Thermal performance modeling of unglazed transpired solar collectors. *J Model Eng* 2018;**16**:391–400.

[23] Saini P, Paolo B, Fiedler F *et al.* Techno-economic analysis of an exhaust air heat pump system assisted by unglazed transpired solar collectors in a Swedish residential cluster. *Sol Energy* 2021;**224**:966–83.

[24] Erenturk S, Erenturk K. Comparisons of novel modeling techniques to analyze thermal performance of unglazed transpired solar collectors. *Measurement* 2018;**116**:412–21.

[25] Nithiarasu P, Lewis RW, Seetharamu KN. *Fundamentals of the Finite Element Method for Heat and Mass Transfer*. John Wiley & Sons, 2016.

[26] Safijahanshahi E, Salmanzadeh M. Performance simulation of combined heat pump with unglazed transpired solar collector. *Sol Energy* 2019;**180**:575–93.

[27] Hollick JC. Commercial scale solar drying. *Renew Energy* 1999;**16**:714–9.

[28] Leon MA, Kumar S. Mathematical modeling and thermal performance analysis of unglazed transpired solar collectors. *Sol Energy* 2007;**81**:62–75.